Long-term behaviour of an instrumented wall reinforced with geogrids

P. Carrubba
University of Padova, Italy

N. Moraci
University of Reggio Calabria, Italy

F. MontanellI
Tenax S.p.A., Viganò Brianza, Lecco, Italy

Keywords: Reinforcement, Walls, Monitoring, Creep.

ABSTRACT: A 4m height vertical retaining wall, 10 m long, has been constructed more than two years ago by reinforcing the backfill with two different kinds of geogrids: one-directional and bi-directional geogrids, covering two section of 5m of wall with different vertical spacing and length of anchorage.
The wall was designed with a safety factor close to unit and has been surcharged up to failure with an additional 3.5 m of backfill, within the end of 1997, thus doubling the original height of the wall. In order to control the static behaviour of the reinforced structure in the elapsed time after completion, instrumentation has been installed inside the wall. Geotechnical characterisation of the constituent element of the wall has been carried out by means of in situ and in laboratory tests.
More than 16000 hours of data have been collected and analysed in terms of reinforcement deformations and displacements in time, variation of vertical pressure in soil with temperature, rainfall and loading sequences.
The aim of this study is to better understand the long term behaviour of the reinforced structure.

1 INTRODUCTION

A vertical retaining wall, 4 m high and 10 m long, was constructed by reinforcing the backfill with two different types of geogrids. Reinforcements were instrumented with strain gauges, tensile load transducers and horizontal displacement sensors.

Total pressure transducers were also installed inside the wall to properly monitor the vertical stress acting at the reinforcement levels.

The structure was monitored starting from the early phase of construction until failure, which was induced by surcharging the wall with 3.5 m of backfill. Data were collected over a period of about 16,000 hours.

The aim of this research is to better understand the behaviour of reinforced structures in time, with particular reference to the evolution of stress and strain along reinforcements.

2 SOIL AND GEOSYNTHETIC PROPERTIES

This paper deals with previously published data (Carrubba et al., 1999) about a reinforced wall located in Cereda, near the town of Vicenza (Italy).

The structure, was built by means of a quarry tout-venant, with uniformity coefficient $C_U = 130$ and curvature coefficient $C_C = 19$. The fine fraction, about 10 % in weight, has a liquid limit $W_L = 28$, a plastic limit $W_P = 20$ and a plasticity index PI = 8. According to the Unified Soil Classification System, this soil was classified as a clayey gravel (GC).

Laboratory compaction tests were carried out following both the standard and the modified AASHTO. The maximum dry unit weight values were $\gamma_{d\ max}$ = 20.95 kN/m^3 and $\gamma_{d\ max}$ = 22.25 kN/m^3, with the associated optimum water contents of W_{opt} = 8.5% and W_{opt} = 5.5% respectively. In situ evaluation of the unit soil weight gave a mean value of γ = 17.7 kN/m^3, showing a lower degree of compaction in comparison with laboratory results (about 80% and 84% of the modified and the standard density respectively). Permeability was evaluated by means of constant hydraulic tests performed in triaxial cell under confining pressures of 50 kPa and 100 kPa. The tests, carried out on large diameter compacted samples (∅ = 100 mm), gave permeability coefficients ranging from 2.0 10^{-4} cm/s to 2.5 10^{-4} cm/s.

Soil shear strength was investigated by means of consolidated-drained triaxial tests performed on large diameter specimens. Due to the dilatant nature of the compacted soil, the tests indicated a very high shear strength under confining stresses σ_c varying between 20 kPa and 100 kPa. According to Mohr-Coulomb failure criterion, the following mean shear strength parameters were selected: friction angle φ' = 46.5° and cohesion c' = 15.0 kPa. The soil modulus was obtained from unloading-reloading cycles in triaxial tests and a mean value of E' = 50,000 kPa was selected. The at-rest soil pressure coefficient K_0 = 0.4 was obtained by means of drained triaxial compression tests under controlled horizontal strain.

The wall was built using two different geogrids. One section of the wall, 5.0 m wide, was reinforced with 3 layers, 2.0 m long, of a high-density polyethylene (HDPE) uniaxial oriented extruded geogrids (GG45PE). The second section of the wall, 5.0 m wide, was reinforced with 3 layers, 2.2 m long, of a polypropylene (PP) biaxially oriented extruded geogrids (GG20PP).

According to current ASTM and CEN draft methodologies, large scale pull-out tests were performed in laboratory on wide width geogrids (1 m long and 0.5 m wide). Interaction factors, f_{po} close to unit were obtained for both the geosynthetic types.
The nominal properties of reinforcements are reported in Table 1.

3 DESIGN AND CONSTRUCTION

The reinforced wall was designed using the limit equilibrium approach implemented in the RESLOPE code (Leshchinsky 1995). The two sections of the wall were designed according to different failure mechanisms: the tie-back tensile failure, for the wall reinforced with GG20PP geogrids, and the pullout failure for the other wall reinforced with GG45PE geogrids (Fig. 1).

All the safety and the material factors were considered equal to 1.00, to achieve failure under the maximum surcharge. The long term tensile strength of the geogrids was assumed to be coincident with the peak tensile strength, evaluated by means of wide width tensile tests (ASTM D4595).

Based upon the design strength, different vertical spacing were obtained for the two geogrid types. For the section reinforced with GG20PP geogrids, three layers 2.20 m long were employed. The first layer was installed at elevation 0.00 m with respect to the base, the second at 0.80 m and the third at 2.40 m.

For the section reinforced with GG45PE geogrids, three layers 2.00 m long were employed. The first layer was installed at elevation 0.00 m with respect to the base, the second at 1.30 m and the third at 2.90 m.

To ensure the face stability, the walls were constructed using “left in place” welded wire formworks. These are wire mesh (∅ = 8 mm, # 200 × 200 mm) 1.5 m in height, forming an angle of 85° with the horizontal. The soil was compacted in layers of 0.3 m in thickness, using a vibrating roller.

Table 1. Geogrids nominal properties.

Product Name	Tenax LBO 220 SAMP	Tenax TT 201 SAMP
Product Code	GG20PP	GG45PE
Polymer Type	PP	HDPE
Nominal Tensile Strength	20 kN/m	45 kN/m
Strain at Peak	11%	12%
Tensile Strength at 2% Strain	7 kN/m	13 kN/m
Tensile Strength at 5% Strain	14 kN/m	26 kN/m
Unit Weight	270 g/m^2	450 g/m^2
Mesh Sizes	41×31 mm	130×15 mm
Junction Strength	18 kN/m	36 kN/m

The geogrids were instrumented with self-temperature compensated strain gauges having a nominal gauge length of 5 mm, a maximum strain limit of 10 % and a measurement accuracy of 0.5 %. Ten strain gauges were installed on each reinforcement at a spacing of about 0.20 m and all the instrumentation was connected to an automatic acquisition system. The location of strain gauges wit respect to the face are reported in Table II.

For both the geogrids, additional specimens were instrumented with strain gauges and tested in the laboratory to obtain the conversion factor between the strain gauges measurements and the actual strain. The stress-strain curves and the conversion factor were analysed as function of time, temperature and stress level. The following tests were performed to define the in isolation time dependent properties of the geogrids: single rib tensile tests, low strain rate tensile tests and creep tests under different load ratios and temperatures.

Three inox steel tensile load cells, similar in shape to the uniaxial geogrid, were connected to each GG45PE reinforcement to measure and record the actual tensile loads acting on each layer. These load cells were constructed using a steel metal plate, 2 mm thick, with oval apertures of 220 mm.

Three vertical total stress cells, having a diameter of 300 mm, were installed in soil mass at each GG45PE reinforcement elevation to record the actual total vertical stress. These cells were located 1.0 m behind the wall face.

Horizontal multiple base displacements sensors were installed on the GG45PE geogrids to monitor the absolute and the differential displacements of the reinforced mass.

The wall was built in one week and left to rest for about 75 days. Therefore, it was surcharged every 75 days with soil layers of about 1.0 m in thickness, until an overall height of 7.5 m was reached. Data were recorded up to 16,000 hours.

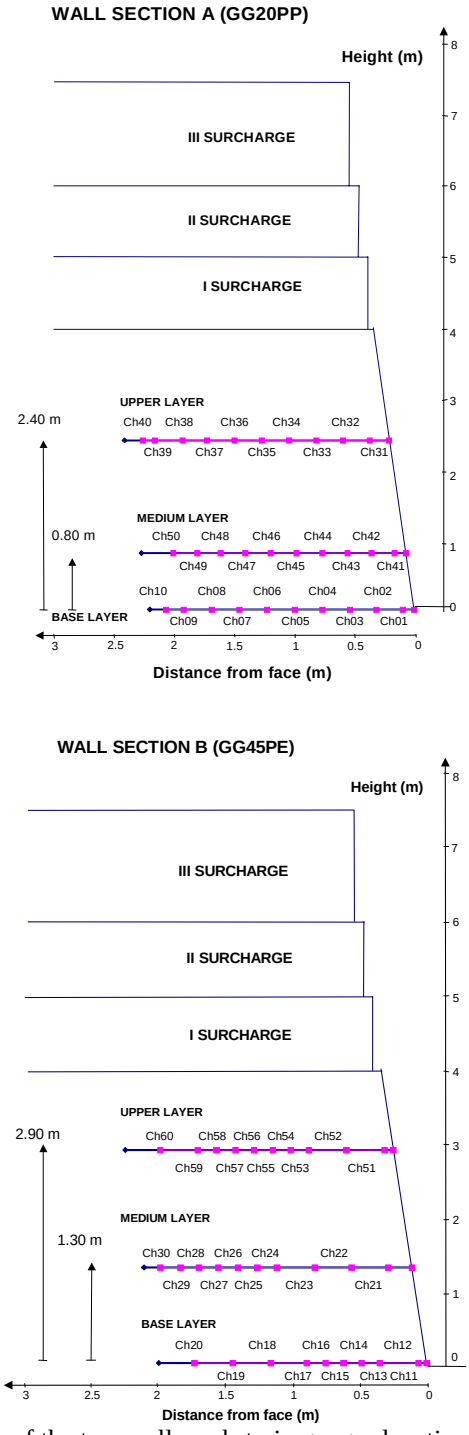

Figure 1. Cross sections of the two walls and strain gauges location along reinforcements.

4 ANALYSIS OF THE RECORDED DATA

Fig. 2 and 3 show the development of tensile strain over time in all the reinforcing layers respectively for GG20PP and GG45PE geogrids.

These data indicate that tensile strain is mainly dependent on stress level achieved during surcharging, but also geogrid type and creep properties are influent.

As shown by the diagrams, the creep rate become more evident as surcharge and time increase; moreover, it is more significant for GG20PP, in which the load ratio level is close to 100 %, rather than for GG45PE geogrids with a load ratio level of 45 %.

Table II. Strain gauges location along reinforcements

Wall Section A (Geogrids GG20PP) Channel Number Vs. Face Distance						**Wall Section B** (Geogrids GG45PE) Channel Number Vs. Face Distance					
Base Layer		**Medium Layer**		**Upper Layer**		**Base Layer**		**Medium Layer**		**Upper Layer**	
Ch.	From Face (m)	Ch.	From Face (m)	Ch.	*From Face (m)*	Ch.	From Face (m)	Ch.	*From Face (m)*	Ch.	From Face (m)
01	0.095	**41**	0.095	**31**	0.160	**11**	0.060	**21**	0.175	**51**	0.065
02	0.315	**42**	0.285	**32**	0.385	**12**	0.205	**22**	0.450	**52**	0.350
03	0.535	**43**	0.485	**33**	0.605	**13**	0.350	**23**	0.725	**53**	0.630
04	0.765	**44**	0.695	**34**	0.830	**14**	0.485	**24**	1.010	**54**	0.765
05	0.995	**45**	0.910	**35**	1.060	**15**	0.620	**25**	1.155	**55**	0.900
06	1.225	**46**	1.125	**36**	1.285	**16**	0.755	**26**	1.300	**56**	1.040
07	1.455	**47**	1.335	**37**	1.515	**17**	0.895	**27**	1.445	**57**	1.180
08	1.685	**48**	1.540	**38**	1.720	**18**	1.165	**28**	1.590	**58**	1.320
09	1.920	**49**	1.735	**39**	1.950	**19**	1.450	**29**	1.730	**59**	1.460
10	2.055	**50**	1.935	**40**	2.050	**20**	1.735	**30**	1.880	**60**	1.740

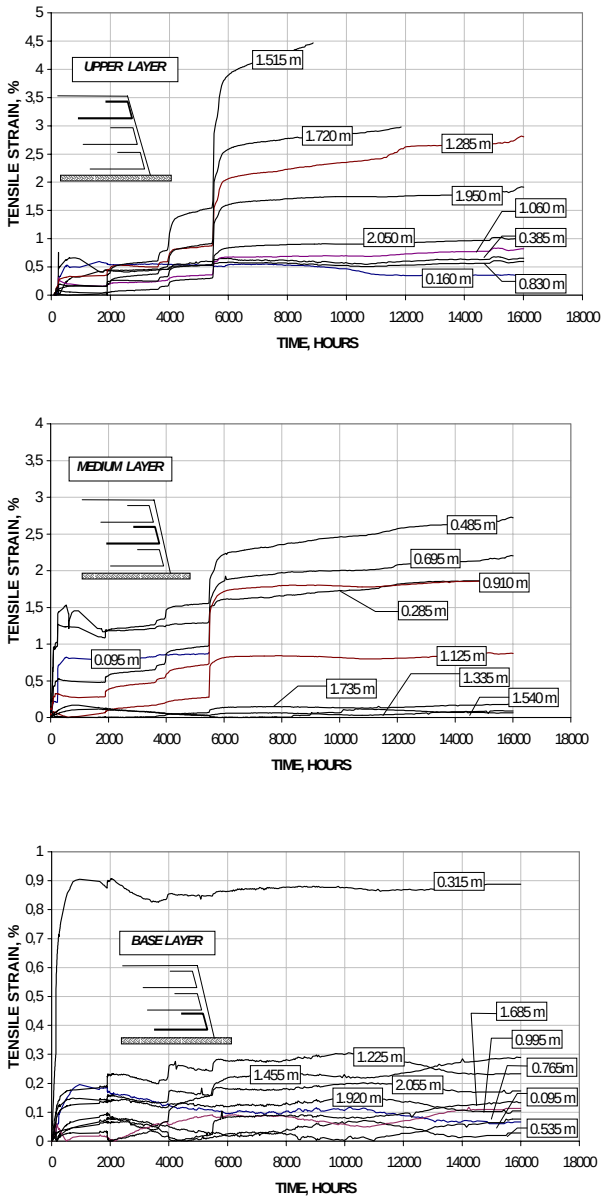

Figure 2. Tensile strains vs. time for the GG20PP geogrids.
Curves are labelled according to the strain gauges face distance.

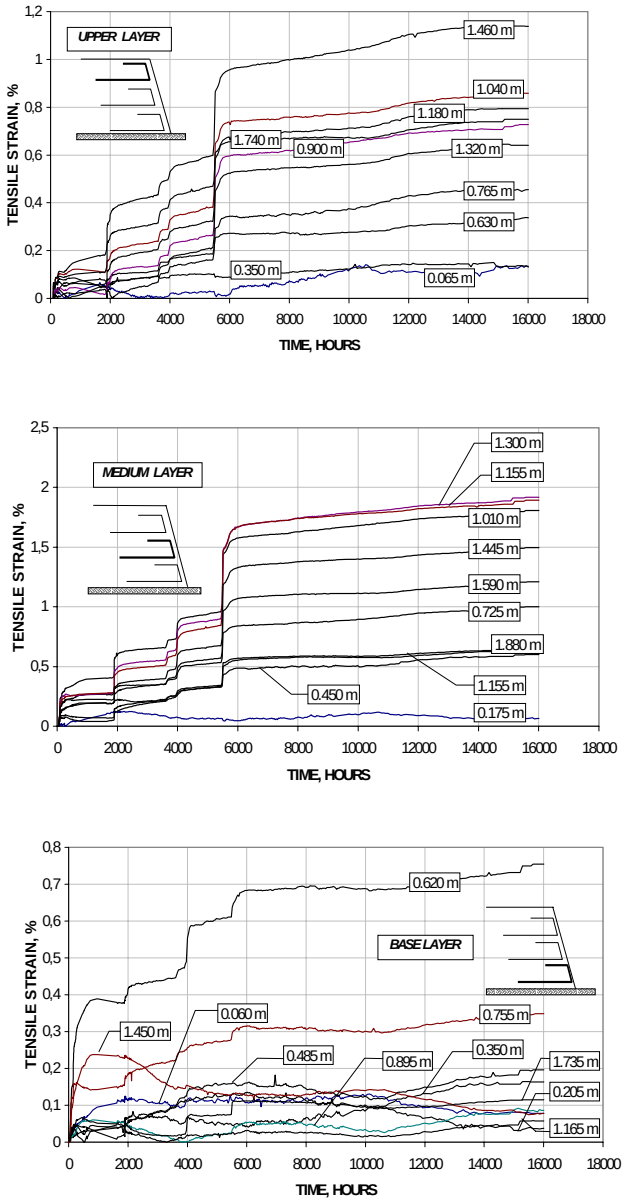

Figure 3. Tensile strains vs. time for the GG45PE geogrids.
Curves are labelled according to the strain gauges face distance.

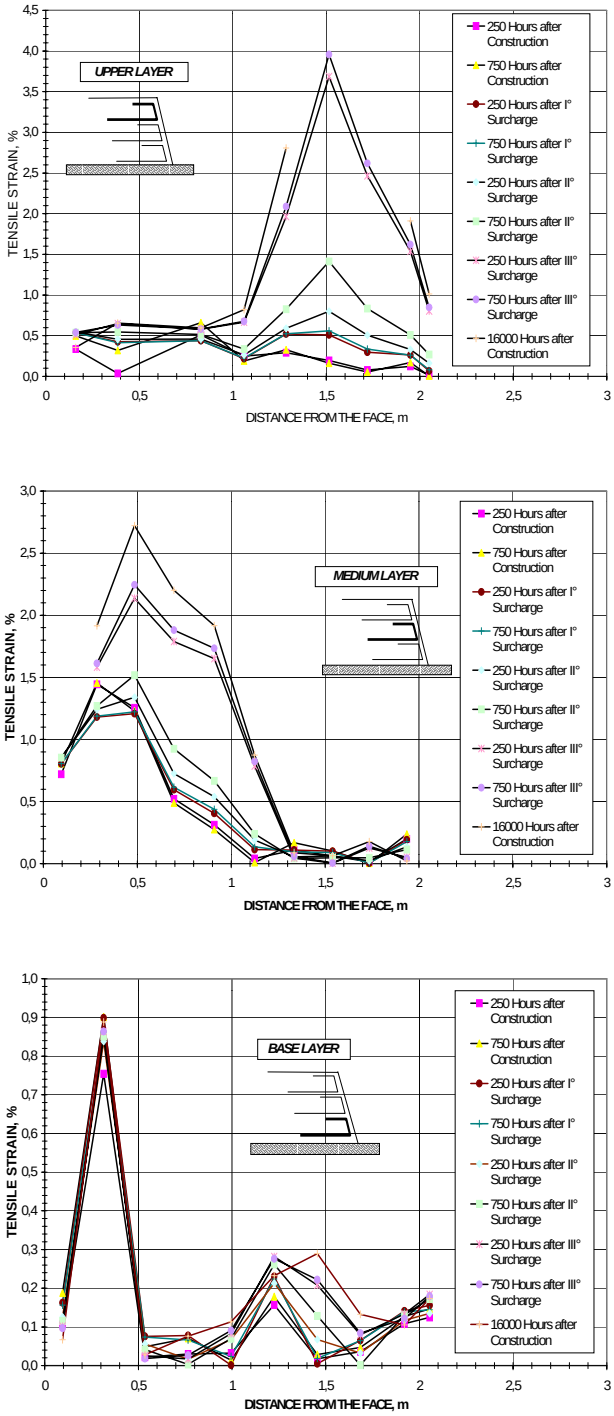

Figure. 4. Tensile strains vs. distance from the face along the GG20PP geogrids. Curves are represented for different times.

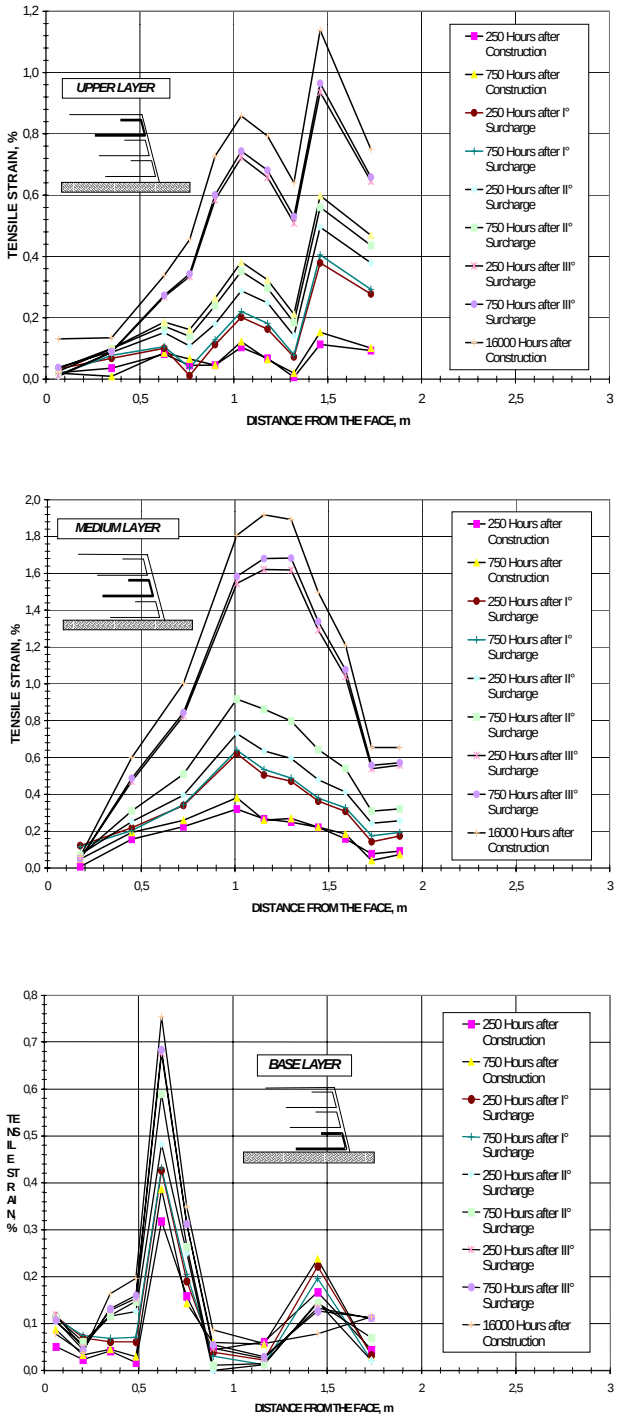

Figure. 5. Tensile strains vs. distance from the face along the GG45PE geogrids. Curves are represented for different times.

The development of tensile strains versus time, for strain gauges located at different positions along the geogrid length, is shown in Figg. 4 and 5 for both GG20PP and GG45PE geogrids.

The above figures show also the location of maximum tensile strain achieved in each reinforcement. Using this information it has been possible to determine the location of the failure surfaces and comparisons have been carried out with the results of numerical methods (Biondi et al. 2000).
The failure mechanism for GG20PP is of ultimate tensile strength in the upper reinforcing layer (tieback failure), as shown in Fig. 4 by the high values of measured tensile strain (more than 4.0 %). The mechanism of failure for GG45PE is of pullout of the upper and the medium reinforcement; in this case lower values of the measured tensile strains (ranging between 1.0 % and 2.0 %) have been observed (Fig. 5).
The creep properties for the two types of reinforcements during the period of observation have been studied in terms of strain rate under constant tensile stress. For this purpose, the strains occurred during the third step of surcharging have been considered.

The strain rate has been evaluated by means of the following expression:

$$\dot{\varepsilon} = \frac{\Delta\varepsilon\%}{\Delta t} \qquad \left[\frac{\%}{\text{year}}\right] \qquad (1)$$

Finally, strain rate has been correlated to the level of tensile strain achieved in the reinforcements (Table III).

Table III. Correlation between tensile strain and strain rate in reinforcements.

$\varepsilon\%$	$\dot{\varepsilon} = \frac{\Delta\varepsilon\%}{\Delta t}$ $\left[\frac{\%}{\text{year}}\right]$	
	Geogrids GG20PP	Geogrids GG45PE
0.50	0.00	0.10
0.75	0.00	0.15
1.00	0.20	0.15
1.50	0.35	0.20
2.00	0.50	-
2.50	0.70	-
4.00	1.25	-

From Figg. 2 and 3, it is possible to observe that creep has been stable and constant in the elapsed time for all the reinforcements and that strain rate linearly increases with the level of tensile strain. The only exception is for the upper layer of geogrid GG20PP, at 1.515 m from face: in this zone the level of strain, of about 4 %, may induce unstable creep with associated large extension of the geogrid This evidence is congruent with the failure mode designed for the wall.

5 CONCLUSION

Two sections of a vertical retaining wall, 4 m high and 10 m long, were built by reinforcing the backfill with two different geogrids. The reinforcing layers were instrumented for long term observations of tensile strain. The walls were carried up to failure by surcharging them with 3.50 m of backfill.

The collected values of tensile strains along reinforcements allowed a clear location of the failure surfaces. Two different failure mechanisms were identified: a pullout failure for the GG45PE

reinforced wall, and a tensile failure for the GG20PP reinforced wall.

Monitoring was successful throughout the whole time of observation (16.000 hours) and allowed the evaluation of the creep effects in geosynthetics. Creep has been stable and constant in the elapsed time for all the reinforcements, with strain rate linearly increasing with the level of tensile strain. The only exception is for the upper layer of geogrid GG20PP, at 1.515 m from face: in this zone the level of strain, of about 4 %, may induce unstable creep with associated large extension of the geogrid.

Finally, instrumentation and long term observations of a large scale model, can be still considered a valuable tool in understanding the behavior of soil reinforced walls.

REFERENCES

ASTM D4595-86. 1996. Tensile Properties of Geotextiles by the Wide-Width Strip Method. ASTM, PA, USA.

Biondi, G. Maugeri, M., Carrubba, P. 2000. Numerical modelling of a geogrid reinforced wall. EUROGEO 2000, Second European Geosynthetics Conference, October 15-18, 2000, Bologna, Italy.

CEN. 1997. Geotextiles and geotextile related products. Determination of pull-out resistance in soil. CEN\TC 189, doc N° 284, Dec 1997.

Bonaparte, R., Holtz, R.D. and Giroud, J.P. 1987. Soil reinforcement design using geotextiles and geogrids. Geotextile Testing and the Design Engineer, ASTM STP 952, pp. 69-116.

Carrubba, P., Moraci, N., Montanelli, F. 1999. Instrumented soil reinforced retaining wall: analysis of measurements. Proceeding Geosynthetic ’99, Boston, U.S.A., pp. 921-934.

Jewell, R.A. 1991. Application of revised design charts for steep reinforced slopes. Geotextiles and Geomembranes, Vol.10, n.4, pp.203-233.

Jewell, R.A., Paine, N., Woods, R.I. 1984. Design method for steep reinforced embankments. Polymer Grid Reinforcement in Civil Engineering, Thomas Telford, London, U.K., pp.70-81.

Leshchinsky, D., Perry, E.B. 1987. A design procedure for geotextile-reinforced walls. Proceeding Geosynthetic ’87, New Orleans, U.S.A., pp.95-107.

Leshchinsky, D. 1995. RESLOPE: Design Manual. Department of Civil Engineering, University of Delaware, U.S.A.

Schmertmann, G.R., Chouery-Curtis, V.E., Johnson, R.D. and Bonaparte, R. 1987. Design charts for geogrid-reinforced soil slopes. Proceeding Geosynthetic ’87, New Orleans, U.S.A., pp.108-120.

Simac, M.R., Christopher, B.R., and Bonczkiewicz, C. 1990. Instrumented field performance of a 6 m geogrid soil wall. Proceeding 4th International on Geotextiles Geomembranes and Related Products, The Hagne, Holland, Vol.1, pp.53-59.